

DOI: 10.1002/adfm.200500692

# Self-Assembled Shape-Memory Fibers of Triblock Liquid-Crystal Polymers\*\*

By Samit V. Ahir, Ali Reza Tajbakhsh, and Eugene M. Terentjev\*

New thermoplastic liquid-crystalline elastomers have been synthesized using the telechelic principle of microphase separation in triblock copolymers. The large central block is made of a main-chain nematic polymer renowned for its large spontaneous elongation along the nematic director. The effective crosslinking is established by small terminal blocks formed of terphenyl moieties, which phase separate into semicrystalline micelles acting as multifunctional junction points of the network. The resulting transient network retains the director alignment and shows a significant shape-memory effect, characteristic and exceeding that of covalently bonded nematic elastomers. Its plasticity at temperatures above the nematic–isotropic transition allows drawing thin well-aligned fibers from the melt. The fibers have been characterized and their thermal actuator behavior—reversible contraction of heating and elongation on cooling—has been investigated.

## 1. Introduction

Liquid-crystalline elastomers have demonstrated their unique material properties and potential for applications in a number of areas. They also present challenging problems for fundamental science, ranging from applied mathematics of elastic media with microstructure, to physical effects of shape memory, soft elasticity, and pattern formation, and to new synthetic routes and concepts. One of the most remarkable properties of nematic elastomers formed with the director aligned in a monodomain fashion is uniaxial spontaneous deformation in response to any external factor changing the underlying order parameter. The resulting shape memory is very different from all other shape-memory effects reported in the literature in that it is a fully reversible, equilibrium phenomenon (other shape-memory systems act only in a one-stroke way and require a reset afterwards). It also has astonishingly large amplitude, with deformation exceeding 200–300 %, and can be stimulated by temperature change, irradiation by light, and exposure to solvents. An overview of these effects, related materials, and the history of publications is available in the literature.<sup>[1]</sup>

One of the difficulties that still restricts the broad range of application of nematic-elastomer actuators is the problem of forming the network with a particular alignment of the nematic director. The most common method currently in use is the

technique of two-step crosslinking, pioneered by Küpfer and Finkelmann.<sup>[2]</sup> It is based on first forming a partially crosslinked gel network with no specified director orientation, then mechanically stretching it, thus inducing an aligning internal stress, and then fully crosslinking the network to record the imposed orientation. Most of the (highly successful) work on monodomain nematic elastomers in the last decade has been done on these systems. However, there are two inherent disadvantages in this approach, if it were to be used in any practical application (apart from being a complicated and delicate three-stage process). The initial half-crosslinked polydomain system, aligned by the applied stress, still retains sharp (localized) domain boundaries even though the director in each domain has been uniformly aligned (see Fridrikh and Terentjev<sup>[3]</sup> for detail of polydomain–monodomain transition). These embedded walls of high distortion make the resulting elastomer internally constrained in its mechanical response.<sup>[1]</sup> One cannot reduce the number of random crosslinks established at the first stage because the application of an aligning stress requires a certain mechanical strength of the network, and one cannot overdo the second-stage crosslinking in order to preserve the entropic nature of the final elastomer.

One particularly attractive configuration of the reversible shape-memory polymer system is demonstrated in aligned fibers. The applications of shape-memory fibers with a large stroke and stress of ~100 kPa<sup>[4]</sup> are not only evident in the textile industry, where the smart fabrics and clothing are the obvious outcome—different applications range from surgical technology to “real” artificial muscles made biomimetically using bundles of fibers. However, although the alignment of drawn polymer fibers is easily and commonly achieved, in the case of nematic elastomers one must also achieve chemical crosslinking at early stages after the melt (or solution) extrusion. At the typical speeds of kilometers per minute used in fiber-drawing technology, this appears an impossible task for any chemical reaction. The only example of nematic-elastomer

[\*] Prof. E. M. Terentjev, S. V. Ahir, Dr. A. R. Tajbakhsh  
Cavendish Laboratory, University of Cambridge  
Madingley Road, Cambridge CB3 0HE (UK)  
E-mail: emt1000@cam.ac.uk

[\*\*] This research has been supported by EPSRC, the EC FP6 IP “LEAP-FROG” and Makevale Ltd. We are grateful to T. Peijs and C. Reynolds of Queen Mary University London for help with fiber drawing and access to DSM Xplore extruder.

fiber in the literature<sup>[5]</sup> characteristically uses small, hand-drawn pieces of uncontrolled thickness, held still for the time required for the UV-initiated crosslinking to establish. This is clearly unsuitable for any practical application.

In this paper we follow a different approach to achieve fast linking of the drawn fiber. The principle of thermoplastic elastomers linked by microphase separation of (telechelic) triblock copolymers is well tested in rubber technology. The classical thermoplastic elastomer is based on styrene–isoprene–styrene block copolymers,<sup>[6]</sup> where the aggregated glassy styrene micelles link the network of elastically active isoprene chains. Recently, important advances have been made by incorporating liquid-crystalline polymers as active middle blocks, within such telechelic principles.<sup>[7,8]</sup> In both cases, the active middle block was a side-chain nematic polymer. The micellar phase-separated morphology reported by Kempe and co-workers<sup>[7]</sup> is similar to our work, although the authors used their telechelic gel in an electro-optical cell, at high dilution in low-molar-weight nematic solvent. The free-standing elastomer system reported by Li and co-workers<sup>[8]</sup> had the lamellar or striated morphology.<sup>[9]</sup> Thermal expansion of some 20% was observed. Acrylate groups were included in the triblock chains and UV polymerization was used to permanently fix the structure.

## 2. Results and Discussion

We synthesized a new triblock copolymer with a large central block composed of the main-chain nematic polymer<sup>[10]</sup> that has been extensively used in studies of nematic elastomers and demonstrated very large shape-memory effect.<sup>[4,11]</sup> The large shape change in the main-chain polymer is due to the highly anisotropic conformation it acquires in the nematic phase, with the chain folded into hairpins.<sup>[12,13]</sup> The linking is achieved by aggregation of end blocks, made of terphenyl moieties, phase-separated into small micelles holding several of the mid-block chains in an elastic network. Although the pure terphenyl compound is highly crystalline, at this point we cannot be certain if the aggregated micelles are crystalline or amorphous. However, the microphase separation driven by the nematic transition in the mid-block is fast and reliably reproducible after reheating.

Polarized optical microscopy examination showed the nematic phase up to the nematic–isotropic transition point ( $T_{NI}$ )  $\approx 100$  °C, which was confirmed by DSC (differential scanning calorimetry, Fig. 1). The  $1.75 \text{ J g}^{-1}$  energy of the nematic-to-isotropic transition is a typical value for the latent heat involved in this weak first-order phase transition. The triblock copolymer 4''-[ $\alpha$ -(4-{1-[4'-(undecaneoxy)biphenyl-4-yl-methyl] propyl} phenyl)- $\omega$ -(undecaneoxy) poly[oxydecamethylene-4,4''-biphenyl-(2-ethylethylene-1,4-phenyl) diterphenyl dicarboxylate (MCDTE) is a viscous melt above  $T_{NI}$  and an elastic rubber above the glass-transition temperature ( $T_G$ ) of  $\approx 40$  °C. The microphase separation, as

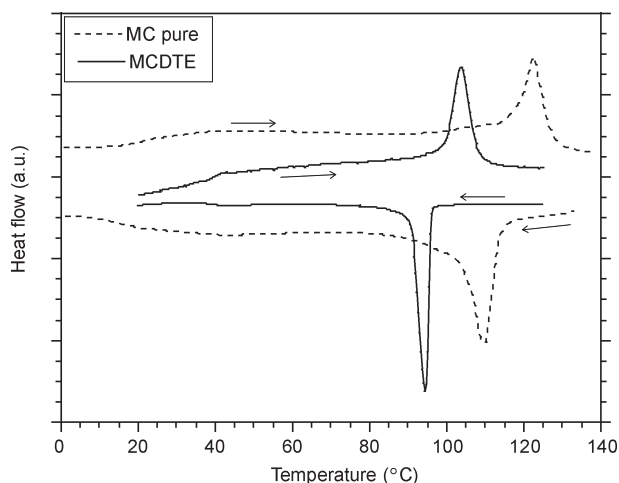


**Figure 1.** The DSC scans on heating and cooling ( $10^\circ\text{C min}^{-1}$ ) showing the nematic–isotropic transitions at  $T_{NI}$  and the glass transitions at  $T_G$ , for the MCDTE (solid lines), and the pure main-chain (MC) nematic polymer (dashed lines) for comparison.

always in such mesogenic systems,<sup>[7,8]</sup> is driven by the nematic order of the large middle block. An important question is that of balancing the rates of aggregation and the rates of polymer melt extrusion. The physical crosslinks (micelles or aggregates) are formed at a certain rate after quenching below  $T_{NI}$ . Adjusting the temperature of this quench and the rate of extrusion/drawing is an empirical process for optimizing the fiber. In our case the fiber extrusion and drawing has been performed with a DSM Xplore-15, from batches of  $\sim 7$  g of the polymer melt. The optimal thermal regime at the extrusion die (1 mm diameter) was  $70^\circ\text{C}$  at a drawing speed of  $\sim 3 \text{ m min}^{-1}$ . Our aim was to produce a substantial length of uniform-thickness fiber, with the nematic director fully aligned along its axis. Figure 2 demonstrates this result, with a roll of long fiber of diameter  $\sim 0.2$  mm (the diameter strongly depends on drawing speed). The resulting aligned thermoplastic elastomer had a Young's modulus  $E \approx 10.7 \text{ MPa}$  at  $40^\circ\text{C}$  and  $E \approx 4.8 \text{ MPa}$  at  $50^\circ\text{C}$ .

Fundamentally, the shape-memory response of the nematic elastomer fiber is much stronger than anything so far reported in the literature. Figure 3 shows the change in length of a piece of fiber suspended with a very small weight ( $> 0.1$  g) to

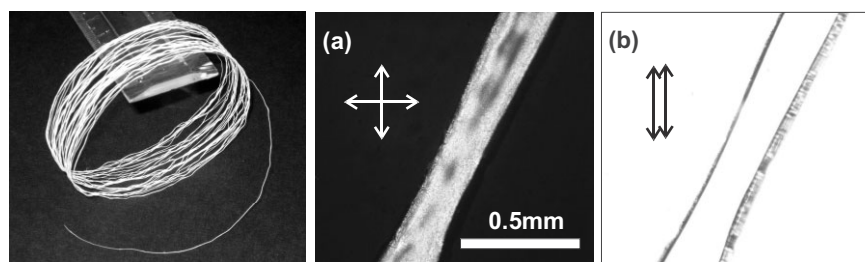


**Figure 2.** The overall picture of a roll of drawn fiber of MCDTE, and two polarized optical microscope images of a fiber, viewed between crossed (a) and parallel polars (b). The director orientation along the fiber is clearly illustrated, as is its overall optical transparency in the aligned nematic state.

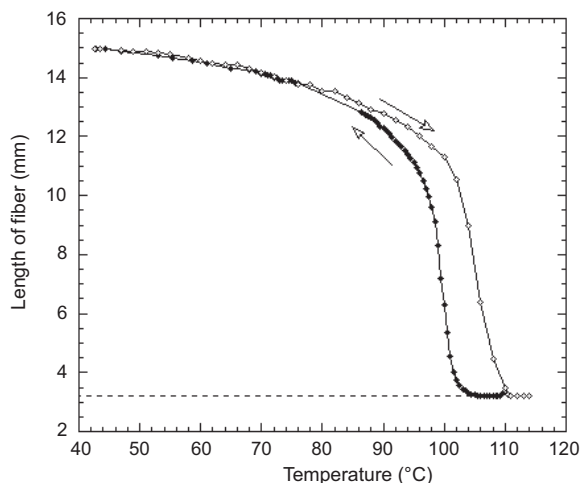


**Figure 3.** The principal, reversible shape-memory effect: changing the length of a freely suspended fiber during a heating and cooling cycle.

prevent curling. This large change in underlying chain anisotropy is certainly due to the high degree of alignment and the material uniformity down to the network-mesh level. This alignment and uniformity are achieved because the nematic ordering and the telechelic crosslinking take place simultaneously (in effect, one driven by the other) during the high shear of fiber drawing. It is in contrast to the imperfect alignment achieved in the traditional two-step crosslinking process in the bulk. An important question in such a thermal-actuation experiment is that of heating/cooling rates. In Figure 3, and in all other analogous measurements in subsequent plots, these rates were kept (very approximately) at  $0.5\text{ }^{\circ}\text{C min}^{-1}$  in order to keep the measurements comparable. One should note that experience with thermal actuation in nematic elastomers has firmly indicated that the limiting factor for the material response rate is the thermal diffusion, or the speed at which the temperature change is delivered to the material. Obviously with thin fibers this thermal diffu-

sion time can be quite short and so the response is correspondingly quite fast.

We next investigated the thermoplasticity of our fibers. It is obvious that if we heat the sample to a temperature far below  $T_{\text{NI}}$ , which is also the temperature of terminal group remixing, or melting of the micellar “crosslinks” of terphenyl groups, then very little creep would occur in the material. Figure 4a confirms this expectation, showing the reversible shape-memory contraction/expansion cycles. Figure 4b shows the same experiment conducted with a fiber holding a weight  $\approx 0.18\text{ g}$ , which corresponds to an extensional stress of  $\sim 60\text{ kPa}$  when converted with the cross-sectional area of a fiber of diameter  $\sim 0.2\text{ mm}$ . We clearly see small thermoplastic creep in each consecutive thermal cycle, which is a recognized characteristic of telechelic systems and other transient networks. Finally, we allowed the repeated thermal cycles to reach higher temperatures, just below and just above the clearing point,  $T_{\text{NI}}$ . As Figure 5 illustrates, the thermoplastic creep at each cycle is noticeable even for a fiber under almost its own weight (we applied a very small weight in all cases to prevent curling).

### 3. Conclusions

The amplitude of actuation strain increases dramatically with the temperature range and reaches the maximum demonstrated in Figure 5b, which corresponds to the full range between  $T_{\text{G}}$  and  $T_{\text{NI}}$  and is about 500%. It is quite remarkable, and deserves special attention, that at  $T > T_{\text{NI}}$  (in the isotropic phase) we appear to always recover the same length of the fiber, which is also seen in Figure 3. This is a point for which we are not ready to offer an explanation: if a normal plastic creep was taking place, the isotropic length should be increasing as well. What we currently observe is more consistent with the assumption that the phase-separated micelles, crystallized at  $T < T_{\text{NI}}$ , take a long time to remix at higher temperatures, while in our thermal cycles the sample spent a relatively short time at high

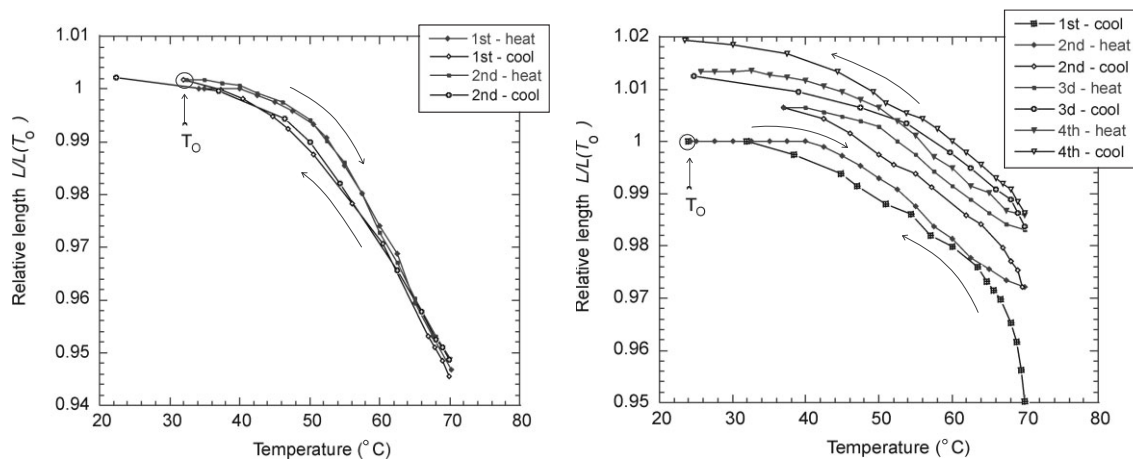


**Figure 4.** a) Heating and cooling of the fiber up to  $70\text{ }^{\circ}\text{C}$  results in the fully reversible shape change: contraction and elongation along the director axis. b) The same experiment carried out with a weight ( $0.18\text{ g}$ , stress  $\sim 60\text{ kPa}$ ), shows the transient thermoplastic flow on each repeated cycle. The initial fiber length at room temperature (labeled  $T_0$ ) is taken as unity and all plots show the relative changes with respect to this length  $L(T_0)$ .

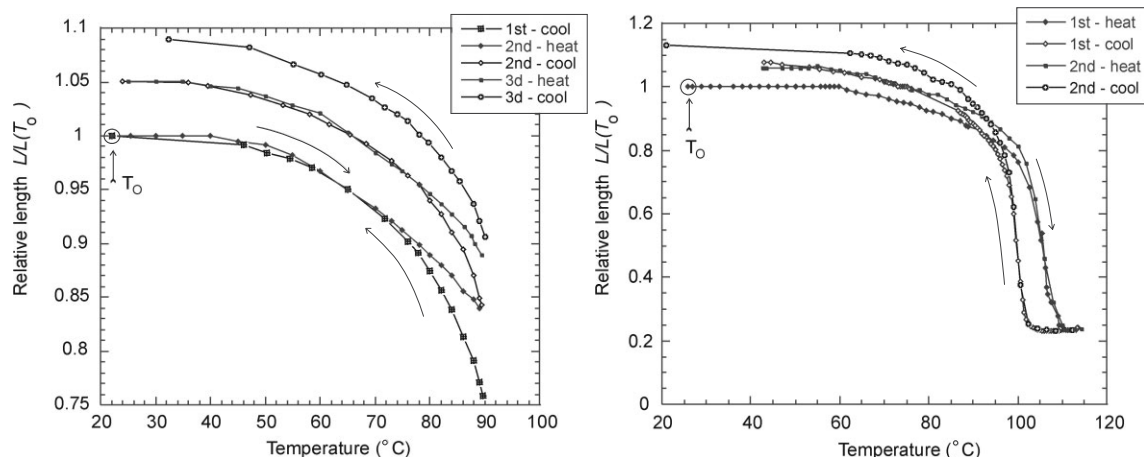


**Figure 5.** a) Heating cycles to 90 °C show elements of thermoplastic flow (or creep) even under the sample's own weight. b) Heating cycles to the isotropic phase show some flow on each step, but also the unambiguous shape-memory effect with a reproducible plateau above  $T_{Ni}$ . The overall length change is ~ 500 %.

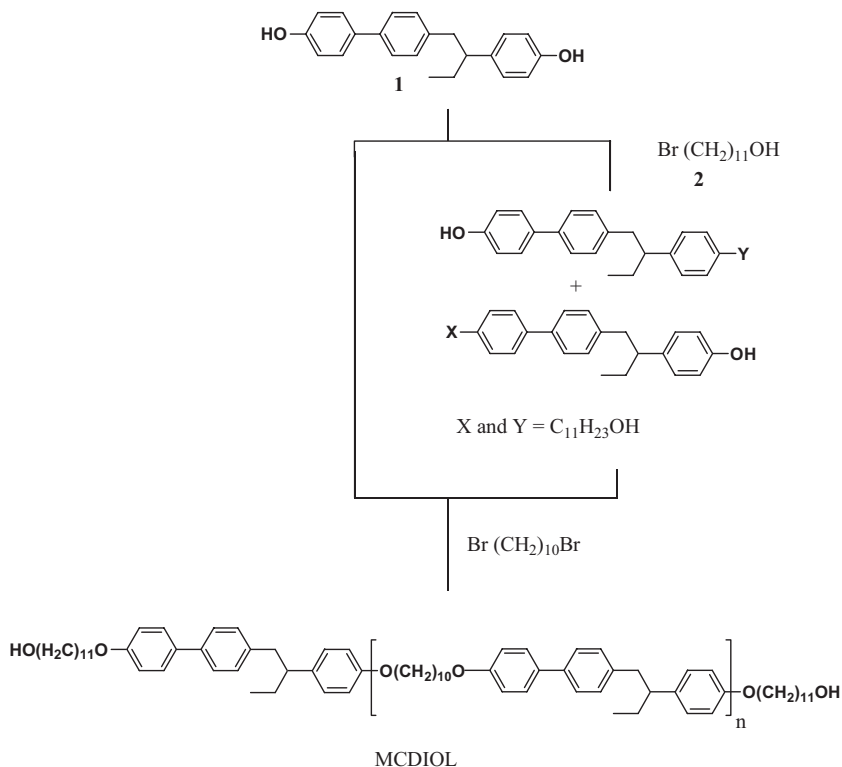
temperature and such a process was not allowed to take place. In any case, it is clear (and well-pointed out previously<sup>[7]</sup>) that for practical applications it is beneficial to incorporate the chemical crosslinking option in phase-separated micelles (e.g., by including acrylate groups ready for UV polymerization). Another practically important variation would be to incorporate photochromic groups (e.g., azobenzene moieties) to achieve photo-stimulated shape memory. Our main aim in this work was to demonstrate the efficiency of fiber extrusion and drawing alignment, and the profound shape-memory effect of self-assembled telechelic networks with the active middle block of main-chain nematic polymer. This was successfully achieved, as shown in Figure 2, while the high degree of nematic alignment achieved at the drawing/self-assembly stage has resulted in record magnitudes of uniaxial, reversible thermal shape memory.

#### 4. Experimental

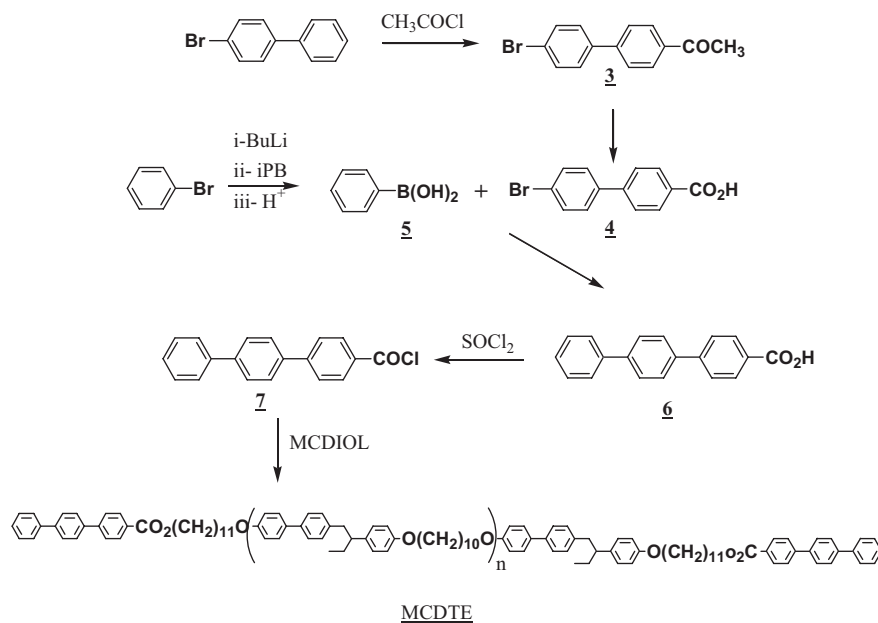
**Preparation of Triblock Copolymer 4<sup>'''</sup>**-[ $\alpha$ -(4-[1-[4'-(undecanoxy)biphenyl-4-ylmethyl] propyl] phenyl)- $\omega$ -(undecanoxy) poly[oxydecamethylene-4,4'-biphenyl-(2-ethylethylene-1,4-phenyl) diterphenyl dicarboxylate (MCDTE)]: The starting material 1-(4-hydroxy-4'-biphenyl)-2-(4-hydroxyphenyl)butane, **1**, was synthesized following the procedures of Percec and Kawasumi [10]. The  $\alpha$ -(4-[1-[4'-(11-hydroxy undecanoxy)-biphenyl-4-ylmethyl]propyl]phenyl)- $\omega$ -(11-hydroxy undecanoxy) poly[oxydecamethyleneoxy-4,4'-biphenyl-(2-ethylethylene-1,4-phenyl), (MCDIOL), was prepared using a modification of Finkelmann process [10,14], see Scheme 1. Compound **1** was alkylated in absolute ethanol (EtOH) overnight with 10-bromoundecane-1-ol (**2**) under reflux conditions. After work-up, the residue oil contained starting material and two isomers, X and Y. The isomers X and Y were separated by column chromatography on silica gel using dichloromethane (DCM) as elu-

ent. MCDIOL was synthesized via phase-transfer-catalyzed polyetherification of compounds **1** and **2** followed by end-capping with the isomers X and Y. The resulting MCDIOL had the average molecular weight of 29 168, which corresponds to an average of  $n=64$  rod-like mesogenic monomers.

The synthetic pathway to terphenyl carboxylic acid to esterify the MCDIOL is outlined in Scheme 2. Friedel-Crafts acylation of commercially available bromobiphenyl using acetyl chloride provided 4-bromobiphenyl acetophenone **3** in good yield. Oxidation of the ketone **3** by sodium hypobromide followed by acidification of the resulting salt, gave the 4-bromobiphenyl-4'-carboxylic acid **4**.



**Scheme 1.** Preparation of MCDIOL.



**Scheme 2.** Preparation of MCDTE.

Bromobenzene was treated with butyllithium at  $-78^{\circ}\text{C}$  for 3 h and then cannulated into a round-bottom flask containing isopropyl borate in tetrahydrofuran (THF, 50 ml). The temperature of the reaction was kept at  $-78^{\circ}\text{C}$  throughout the addition of lithiated benzene. The reaction mixture was allowed to warm to room temperature overnight. Diluted HCl was then added. Continued stirring for 3 h and working-up gave phenyl boronic acid **5**. Suzuki coupling [15] of the boronic acid **5** with the acid **4**, followed by treatment with thionyl chloride gave the terphenyl carboxyl chloride **6**. Esterification of the MCDIOL with the **6** gave the final product, MCDTE (Scheme 2). In total, we produce 5–7 g of the final product in one synthesis, under laboratory-bench conditions.

Received: October 10, 2005  
Final version: November 7, 2005

- [1] M. Warner, E. M. Terentjev, *Liquid Crystal Elastomers*, Oxford University Press, Oxford, UK **2003**.  
[2] J. Küpfer, H. Finkelmann, *Makromol. Chem. Rapid Commun.* **1991**, *12*, 717.

- [3] S. V. Fridrikh, E. M. Terentjev, *Phys. Rev. E* **1999**, *60*, 1847.  
[4] A. R. Tajbakhsh, E. M. Terentjev, *Euro Phys. J. E* **2001**, *6*, 181.  
[5] J. Naciri, A. Srinivasan, H. Jeon, N. Nikolov, P. Keller, B. R. Ratna, *Macromolecules* **2003**, *36*, 8499.  
[6] *Developments in Block Copolymers* (Ed: I. Goodman), Applied Science Publishers Ltd, Oxford, UK **1982**.  
[7] M. D. Kempe, N. R. Scruggs, R. Verduzco, J. Lal, J. A. Kornfield, *Nat. Mater.* **2004**, *3*, 177.  
[8] M. H. Li, P. Keller, J. Y. Yang, P. A. Albouy, *Adv. Mater.* **2004**, *16*, 1922.  
[9] P. G. De Gennes, *Macromol. Symp.* **1997**, *113*, 39.  
[10] V. Percec, M. Kawasumi, *Adv. Mater.* **1992**, *4*, 572.  
[11] G. H. F. Bergmann, H. Finkelmann, V. Percec, M. Zhao, *Macromol. Rapid Commun.* **1997**, *18*, 353.  
[12] X. J. Wang, M. Warner, *J. Phys. A* **1986**, *19*, 2215.  
[13] M. H. Li, A. Brulet, J. P. Cotton, P. Davidson, C. Strazielle, P. Keller, *J. Phys. II* **1994**, *4*, 1843.  
[14] B. Donnio, H. Wermter, H. Finkelmann, *Macromolecules* **2000**, *33*, 7724.  
[15] A. Suzuki, *J. Organomet. Chem.* **1999**, *576*, 147.

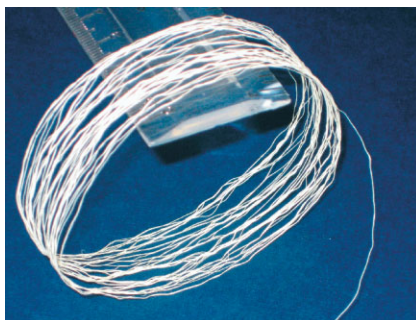


FULL PAPERS

Shape-Memory Polymers

S. V. Ahir, A. R. Tajbakhsh,  
E. M. Terentjev\* ..... ■ – ■

Self-Assembled Shape-Memory Fibers  
of Triblock Liquid-Crystal Polymers



**Telechelic triblock copolymers**, with the dominant middle block a main-chain nematic polymer, provide a self-assembling material for extruding and drawing aligned fibers (see Figure). The resulting thermoplastic elastomer demonstrates reversible shape memory, contracting and elongating by over 500% on temperature change.